# Long-term photometry of the symbiotic nova V1329 Cyg

**D.Chochol**[1], **I.L.Andronov**[2], **V.P.Arkhipova**[3], **L.L.Chinarova**[2], **J.Mattei**[4], **S.Y.Shugarov**[3]

[1] *Astronomical Institute of the Slovak Academy of Sciences 059 60 Tatranská Lomnica, The Slovak Republic*

[2] *Astronomical Observatory, Odessa State University T.G.Shevchenko Park, Odessa 270014, Ukraine*

[3] *Sternberg State Astronomical Institute Universitetskij Prosp. 13, Moscow 119899, Russia*

[4] *American Association of Variable Star Observers, 25 Birch St., Cambridge, MA 02138, USA*

Received: November 10, 1998

**Abstract.** New UBV photometry of the symbiotic nova V1329 Cyg taken in 1988-97 is presented. Long-term postoutburst UBV photoelectric, photographic and visual observations from the AAVSO and AFOEV databases are discussed. The periodogram analysis using the trigonometric polynomial fit with a linear trend reveals the mean normal epoch of the minimum and the mean best fit period as JD $2446771 \pm 3^{\rm d}$ and $956\overset{\rm d}{.}5 \pm 0\overset{\rm d}{.}6$, respectively. The amplitude of the brightness variations is significantly higher in the U-band ($1\overset{\rm m}{.}6$) than in the B,V and pg bands ($1\overset{\rm m}{.}22$). The largest slope of the mean brightness decrease is in the U-band. The characteristics of the light-curves extremes in different bands are tabulated. The phases of the U,B,V light-curves coincide within the error estimates. A secondary period of $553^{\rm d}$ and a cycle of $\approx 5300^{\rm d}$ are suggested.

**Key words:** stars – binaries – symbiotic – photometry – V1329 Cyg

## 1. Introduction

V1329 Cyg (HBV 475) is a member of the small sub-group of symbiotic novae, also including V1016 Cyg and HM Sge, in which TNR outburst leads to a nebular spectrum (Mürset & Nussbaumer, 1994).

In order to illustrate the general photometric behaviour of V1329 Cyg, the historical photographic light-curve (henceforth LC) is presented in Fig. 1. It was compiled using the data published by Dumortier & Stram (1970), Kohoutek & Bossen (1970), Richter (1972), Hicks (1973), Stienon et al. (1974), Witzigman et al. (1978), Iijima et al. (1981), Munari et al. (1988), Arkhipova & Mandel (1991),

Skopal et al. (1992), Hric et al. (1994). In the years 1891-1964 the pg brightness of the object fluctuated around $15^{\rm m}$, with occasional $2\overset{\rm m}{.}5$ deep decreases, which repeated with a period of 950 - 959 days (Stienon et al., 1974; Grygar et al., 1979; Munari et al., 1988). They were explained as the eclipses of a hot component by a red giant. The nova-like outburst of the object started in 1964. The brightness maximum of $11\overset{\rm m}{.}5$ was reached in October 1966. The brightness decline has been accompanied by wave-like variations with the periodicity found in the pre-outburst data. Schild & Schmid (1997) found the ephemerides, valid for the pre-outburst and post-outburst data as $\mathrm{JD}_{min} = 2\ 427\ 687(\pm 20) + 958.0(\pm 1.8)\times E$ and $\mathrm{JD}_{min} = 2\ 444\ 866(\pm 25) + 955(\pm 15)\times E$, respectively. They adopted the ephemeris $\mathrm{JD}_{min} = 2\ 444\ 890 + 956.5\times E$ valid for both sets of data.

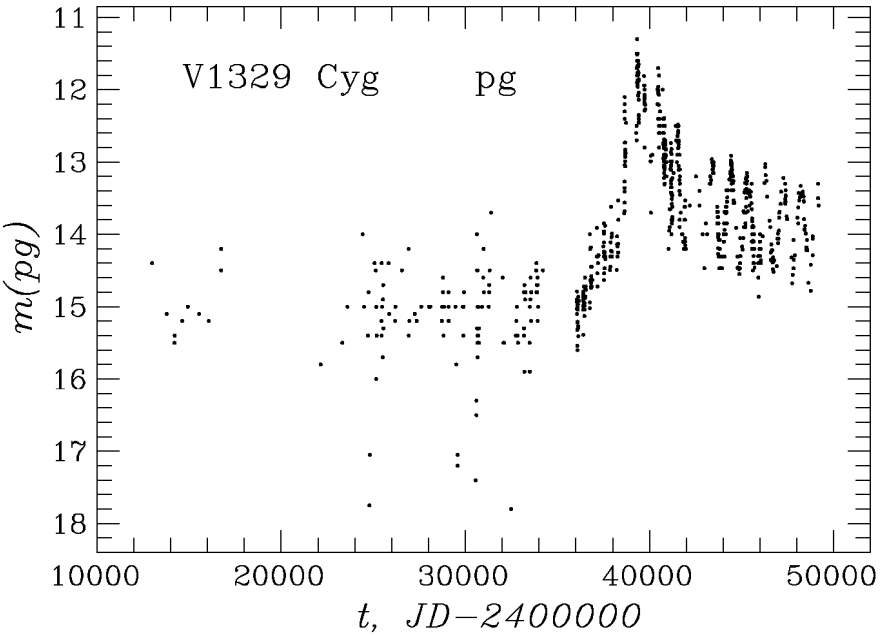


**Figure 1.** The historical photographic LC compiled from published data.

The aim of our paper is to present a new set of U,B,V observations taken in the years 1988-1997 and to perform the period analysis of the post-outburst UBV photoelectric and photographic observations as well as visual estimates of V1329 Cyg from AFOEV and AAVSO databases.

## 2. New observations and data-sets used for the analysis

New photoelectric UBV observations of V1329 Cyg were obtained at the Crimean Station of the Sternberg Astronomical Institute in 1988-1997. A single-channel,

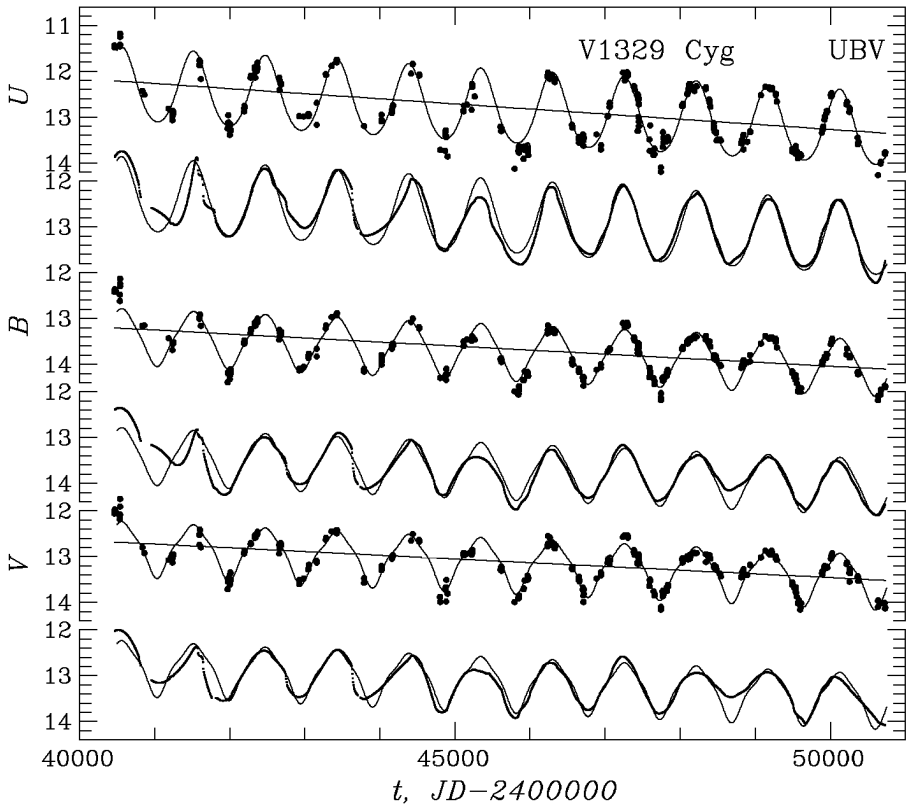


**Figure 2.** The UBV LCs (points) and their approximations by a trigonometric polynomial of order $s = 2$ including a linearly decreasing trend (thin curve) calculated for the data after JD 24420000. The thick curve shows the running parabola (RP) fit with $\Delta t = 400^{\rm d}$ for all data. The declining straight lines show the linear fits using all data.

pulse-counting, photoelectric photometer installed in the Cassegrain focus of the 0.6 m reflector was used. The star BD +35° 4300 (V=9.71, B=9.91, U=10.13) served as the comparison star. Data reduction and atmospheric extinction corrections were carried out in the usual way. As this instrumental system is nearly in agreement with the standard UBV system, the transformation to this system is not necessary (Arkhipova, 1977). Our photoelectric observations taken on 148 nights between Aug. 7, 1988 and Oct. 8, 1997 are in Tab. 6. The U,B,V magnitudes are normal points - mean night averages of the individual observations taken 2-3 times during the night. The mean error of one normal point is $0\overset{\rm m}{.}01$ in B and V and $0\overset{\rm m}{.}02$ in U.

U,B,V LCs of V1329 Cyg compiled from our data as well as data published by Kohoutek & Bossen (1970), Bossen (1972), Arkhipova & Mandel (1973), Arkhipova (1977), Gravina (1985), Taranova & Yudin (1986), Arkhipova & Ikon-

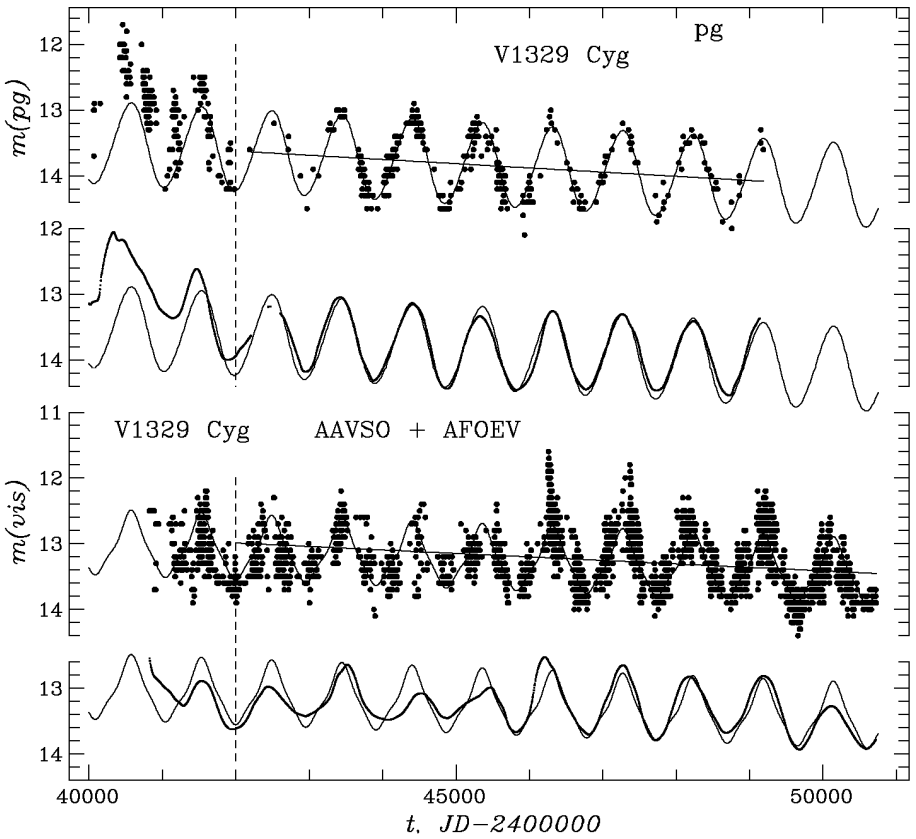


**Figure 3.** The pg and visual LCs (points) and their approximations by a trigonometric polynomial of order $s = 2$ and a linearly decreasing trend (thin curve) calculated for the data after JD 2442000 (vertical dashed line). The thick curve shows the running parabola (RP) fit with $\Delta t = 400^{\rm d}$. The declining straight lines show the linear fits.

nikova (1989), Dapergolas et al. (1991) are shown in Fig. 2.

Visual data consisted of 3173 and 2323 observations from the AAVSO and AFOEV (Schweitzer, 1997) databases, respectively. A significant part of the data overlapped, being published in both databases. After removing the "duplicates", "unsure" (:) and "fainter than" (<) data, a total of 4024 original visual (vis) estimates remained. As shown in Fig. 3, the photographic and visual LCs of V1329 Cyg are characterized by a rapid decline with some superimposed outbursts before JD 2442000. After this date, the mean slope decreased and the LCs started to exhibit wave-like periodic variations. The number of "post-outburst" points after this date is $n = 3754$.

Long-term, post-outburst U,B,V photoelectric, photographic and visual light curves were analyzed in detail. The characteristics of the runs: the times of

the first and last observations (in JD–2400000), the number of observations, the range, the sample mean, and the standard deviation from the mean, are summarized in Table 1.

**Table 1.** The characteristics of the data sets in different runs

| band | $t_1$ | $t_n$ | $n$ | range | $\langle m \rangle$ | $\sigma_O$ |
|---|---|---|---|---|---|---|
| U | 40467 | 50730 | 345 | $11\overset{m}{.}2$-$14\overset{m}{.}3$ | $12\overset{m}{.}86$ | $0\overset{m}{.}67$ |
| B | 40467 | 50730 | 350 | $12\overset{m}{.}1$-$14\overset{m}{.}8$ | $13\overset{m}{.}72$ | $0\overset{m}{.}50$ |
| V | 40467 | 50730 | 351 | $11\overset{m}{.}7$-$14\overset{m}{.}2$ | $13\overset{m}{.}16$ | $0\overset{m}{.}47$ |
| pg | 12994 | 49184 | 943 | $11\overset{m}{.}3$-$17\overset{m}{.}8$ | $13\overset{m}{.}82$ | $1\overset{m}{.}00$ |
| vis | 40823 | 50722 | 4024 | $11\overset{m}{.}6$-$14\overset{m}{.}4$ | $13\overset{m}{.}28$ | $0\overset{m}{.}44$ |

## 3. Periodogram analysis with trend

Due to the fact that a slow trend is superimposed on the cyclic luminosity variations, the problem of the period search becomes more complicated. Assuming a polynomial shape of the trend of order $n_p$, one may write an expression

$$m(\bar{t}+\tau) = a_1 + \sum_{k=1}^{s}(a_{2k}\sin(2\pi f k\tau) + a_{2k+1}\cos(2\pi f k\tau)) + \sum_{k=1}^{q} a_{2s+1+k}\,\tau^k. \quad (1)$$

Here we introduce the variable $\tau = t - \bar{t}$ ($\bar{t}$ is the mean of the times of observations) to decrease the degeneracy of the matrix of normal equations (cf. Andronov, 1994). For the fixed frequency $f$ and the degrees $s$ and $q$ of the trigonometric and ordinary polynomial, respectively, the parameters $a_k$, $k = 1, ...1+2s+q$ may be obtained by the least squares method. This is a statistically justified method because all these parameters are determined from a joint system of normal equations.

Another approach is to determine the parameters of the trend and then to search for periodicity in the $O-C$ residuals from the trend. Such a process is similar to "prewhitening" (Wehlau and Leung, 1964). As an example, we have computed the results of the fits for all photoelectric B observations. The linear trend may be written as

$$m_B \;=\; \underset{\pm 2}{13\overset{m}{.}71} \;+\; \underset{\pm 8}{88}\times 10^{-6}\,(t-46280). \quad (2)$$

The sine approximations for the original observations "$O$" and their residuals "$O-C$" from a linear fit (2) correspond to the period $P = 960\overset{d}{.}8 \pm 1\overset{d}{.}6$ "$O$" ($955\overset{d}{.}7 \pm 0\overset{d}{.}9$ "$O-C$"), mean $a_1 = 13\overset{m}{.}76 \pm 0\overset{m}{.}01$ ($0\overset{m}{.}02 \pm 0\overset{m}{.}01$), semiamplitude $r = 0\overset{m}{.}62 \pm 0\overset{m}{.}02$ ($0\overset{m}{.}57 \pm 0\overset{m}{.}01$) and the normal epoch for minimum $JD_{min} = 2446767 \pm 5$ ($2446777 \pm 2$). The parameters of the complete fit (1) coincide with

that of the prewhitened solution within their error estimates: $P = 956\overset{\mathrm{d}}{.}4 \pm 2\overset{\mathrm{d}}{.}6$, $r = 0\overset{\mathrm{m}}{.}59 \pm 0\overset{\mathrm{m}}{.}01$, $JD_{min} = 2446777 \pm 3$, $a_1 = 13\overset{\mathrm{m}}{.}75 \pm 0\overset{\mathrm{m}}{.}01$. This occurs because $\approx 10$ cycles are covered by the data and thus the phases of the observations are distributed relatively homogeneously. However, the linear trend term $a_{2s+2} = (77 \pm 3)\ 10^{-6}$ mag/day in a complete fit differs from the simple linear slope by 14%, and for other data up to $\approx 40\%$.

One may note that the moment of minimum for a sinusoidal wave is shifted compared to a minimum of the "sine+line" function. This shift for V1329 Cyg is $\Delta T_{min} = 1\overset{\mathrm{d}}{.}5$ and is smaller than the statistical error estimates. These errors are much larger for the sine fit of the original data, as the trend disturbs the phase curve.

The residuals of the original data from a best sine fit show a well pronounced trend. However, its value $(72 \pm 3)\ 10^{-6}$ mag/day differs from the fit (2) by 22%. Thus one has to use a complete set of $1 + 2s + q$ equations instead of two sets of equations with $1 + q$ and $1 + 2s$ unknowns. This example shows a bias of the results owed to incomplete models and thus it may be recommended to use high-order models instead of step-by-step "prewhitening".

The best trigonometric polynomial fit with a linear trend was computed for the U,B,V, vis, pg and pg+B data. The trend is close to the linear one not for the complete data set, but for the "post-outburst" data after the stage of rapid decrease of brightness, i.e. after JD 2442000. The parameters of the fits for such restricted data are listed in Table 2. Here the degree of the polynomial trend was set to $q = 1$. The degree of the trigonometric polynomial $s$ (different for each data set) was determined by using the Fischer's criterion with a "false alarm" probability $P_r < 10^{-4}$. This is the probability that the $(s-1)$ -th harmonic of a given amplitude may be obtained, suggesting the signal is a white noise. The value of $P_r$ may be determined by using the equation $P_r(s) = (1 - V_B)^{\eta}$, where $\eta = (n-3-2s-q)/2$, $V_B = 1-\Sigma[s]/\Sigma[s-1]$ and $\Sigma[s]$ is the sum of squares of the residuals from the trigonometric polynomial of order $s$ with the $q$-th order trend. This expression generalizes that of Andronov (1994) for non–zero values of $q$. For a fixed $s$, the periodogram may be computed as $S(f) = \sigma_C^2/\sigma_O^2$, where $\sigma_O^2$ and $\sigma_C^2$ are variances of the original data and the smoothed values at the arguments of observations, respectively. The term $a_{2s+2}$, measured in magnitudes per day, corresponds to a linear trend. The normal epochs $T_{max}$, $T_{min}$ are expressed in JD-2400000. The pg system is close to the B system, thus it is natural to join the "pg+B" data to obtain the longest possible data-set. However, there is a systematic shift $\langle pg - B \rangle = 0\overset{\mathrm{m}}{.}10$, which was taken into account to reduce the B data to the pg system. This shift was determined by comparing the original pg data with a smoothed value of the B LC at corresponding times and vice versa. The smoothing function was obtained by using a "running parabola" fit with an optimal value of the filter half-width $\Delta t = 400^{\mathrm{d}}$ (see Section 4 for a description).

The periodograms for the B data after JD 2442000 are shown in Fig. 4. Run 1 was obtained by removing the linear trend. The highest peak at the periodogram

**Table 2.** Characteristics of the trigonometric polynomial fit with a linear trend for the observations after JD 2442000

| | U | B | V | vis | pg | pg+B |
|---|---|---|---|---|---|---|
| $n$ | 314 | 319 | 320 | 3754 | 392 | 711 |
| $\bar{t}$ | 46785 | 46779 | 46766 | 47726 | 45230 | 45925 |
| $a_1$ | 12.95 | 13.79 | 13.21 | 13.34 | 13.82 | 13.76 |
| $\pm$ | 0.01 | 0.01 | 0.01 | 0.01 | 0.01 | 0.01 |
| $s$ | 2 | 3 | 3 | 3 | 2 | 2 |
| $10^6 a_{2s+2}$ | 100 | 68 | 70 | 42 | 64 | 108 |
| $\pm$ | 4 | 3 | 3 | 2 | 5 | 7 |
| $P$ | 953.9 | 956.0 | 957.8 | 956.3 | 958.9 | 958.2 |
| $\pm$ | 3.9 | 2.5 | 2.4 | 1.9 | 4.8 | 6.4 |
| $T_{max}$ | 46300.0 | 46304.3 | 46298.3 | 46315.0 | 46362.2 | 46328.8 |
| $\pm$ | 3.9 | 6.2 | 5.8 | 3.2 | 5.7 | 5.2 |
| $T_{min}$ | 46778.9 | 46771.7 | 46768.0 | 46778.9 | 46762.1 | 46755.5 |
| $\pm$ | 10.5 | 4.5 | 3.3 | 4.9 | 5.8 | 4.5 |
| $M-m$ | 0.498 | 0.511 | 0.510 | 0.515 | 0.540 | 0.555 |
| $\pm$ | 0.014 | 0.006 | 0.006 | 0.005 | 0.011 | 0.009 |
| $\Delta m$ | 1.598 | 1.234 | 1.211 | 1.007 | 1.260 | 1.269 |
| $\pm$ | 0.022 | 0.018 | 0.017 | 0.013 | 0.019 | 0.016 |
| $\sigma_{O-C}$ | 0.170 | 0.107 | 0.105 | 0.275 | 0.151 | 0.134 |

corresponds to $P = 955\overset{\mathrm{d}}{.}7 \pm 1\overset{\mathrm{d}}{.}0$, the value close to that listed in Table 2. Run 2 was computed as the difference between run 1 and the sine fit ($s = 1$, $q = 0$), i.e. consequently prewhitened to a linear trend and a $956^{\mathrm{d}}$ wave. Run 3 was computed as the difference between run 1 and the trigonometric polynomial fit with a statistically significant order $s = 3$. The periodograms of runs 2 and 3 show two prominent peaks at $5300^{\mathrm{d}} \pm 160^{\mathrm{d}}$ ($S(f) = 0.22$ and 0.26, respectively) and $554^{\mathrm{d}} \pm 2^{\mathrm{d}}$ ($S(f) = 0.26$ and 0.26, respectively). The secondary peak is shifted from $581^{\mathrm{d}}$ for run 1 to $555^{\mathrm{d}}$ and $553^{\mathrm{d}}$ for runs 2 and 3, respectively. One may note the significant difference between the values obtained for different runs at the same wavelength that justifies the usage of complete system of the equations (1) instead of step–by–step "prewhitening". The ephemeris for the maximum of the $553^{\mathrm{d}}$ wave is

$$JD_{max} = \underset{\pm 9}{2446711} + \underset{\pm 1\overset{\mathrm{d}}{.}9}{553\overset{\mathrm{d}}{.}1} \times E, \qquad (3)$$

The corresponding phase diagram is shown on Fig. 5. The O-C deviations prewhitened to a linear trend, trigonometric polynomial and a best sine fit with $553\overset{\mathrm{d}}{.}1$ period are depicted on Fig. 6. The $5300^{\mathrm{d}}$ wave is clearly visible. Similar results may be seen in the periodograms for other bands. The mean values and

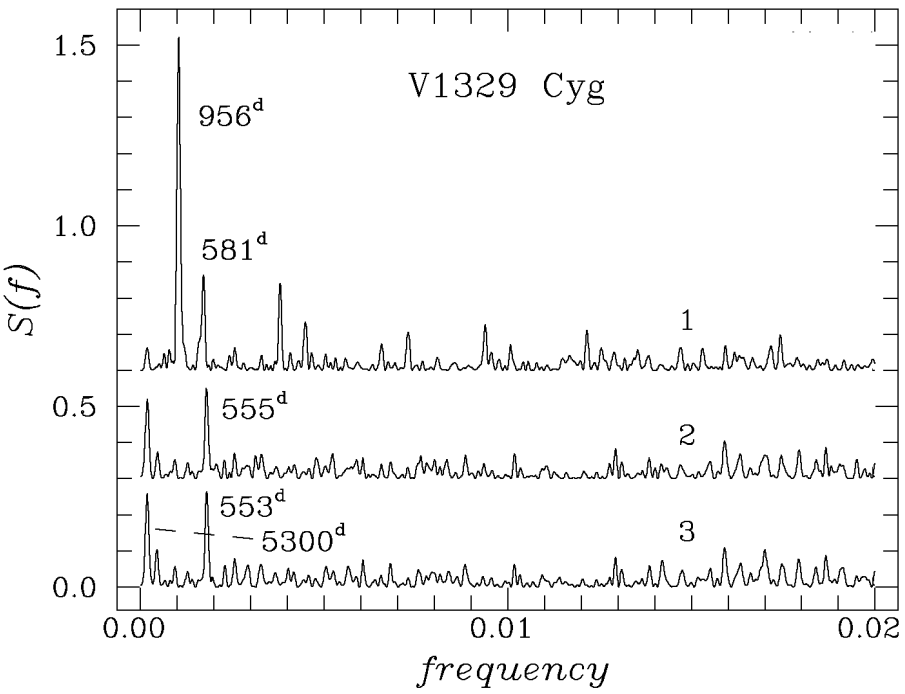


**Figure 4.** The periodograms $S(f)$ for the residuals from the linear "$s = 0$, $q = 1$" fit (1), from the data prewhitened consecutively in respect to the linear trend and best harmonic ($s = 1$) fit (2) and to the best trigonometric polynomial ($s = 3$) fit with a linear trend (3). The periodograms are shifted with a step of 0.3. The photoelectric $B$ observations after JD 2442000 are used.

standard errors in both figures were computed by sampling the data in intervals of equal length.

The semi–amplitude of $554^{\rm d}$ wave in U,B and V is equal to $0\overset{\rm m}{.}075 \pm 0\overset{\rm m}{.}007$, $0\overset{\rm m}{.}077 \pm 0\overset{\rm m}{.}007$ and $0\overset{\rm m}{.}069 \pm 0\overset{\rm m}{.}007$, respectively. Corresponding values of $S(f)$ and $L_p$ are 0.100, 0.264, 0.234 and 4.9, 18.8, 16.0, respectively. The "false alarm" probability is equal to $10^{-L_p}$ (cf. Andronov, 1994). Thus one may conclude that the effective amplitude of such a secondary wave is nearly the same in all bands, but its contribution to U is much smaller than in other bands. The variability is most probably attributed to the hot component, because J,H,K,L photometry do not exhibit clear variational patterns (Nussbaumer & Vogel, 1991). The $554^{\rm d}$ and $5300^{\rm d}$ waves could be explained by systematic changes in both geometry and location of the HII region, which is the main source of the optical continuum as proposed by Skopal (1998).

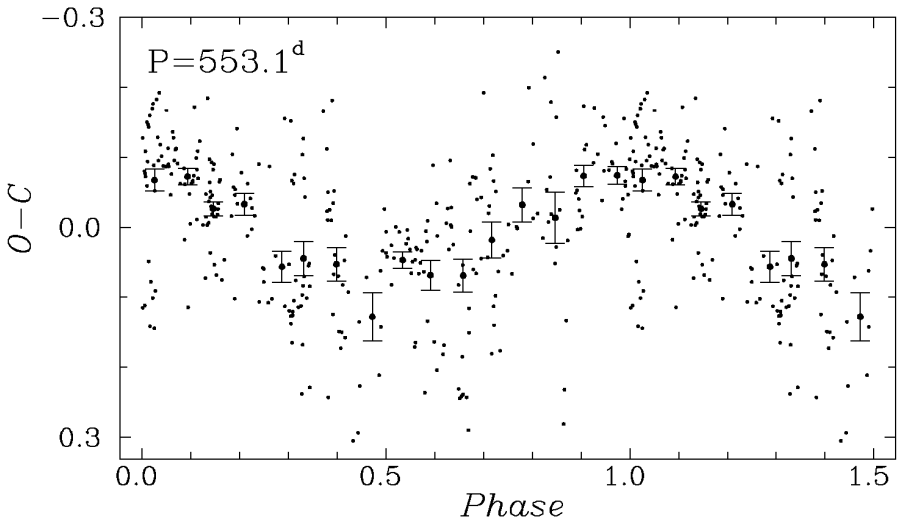


**Figure 5.** The phase diagram for B run 3 according to the ephemeris: $JD_{max} = 2446711 + 553.1 \times E$.

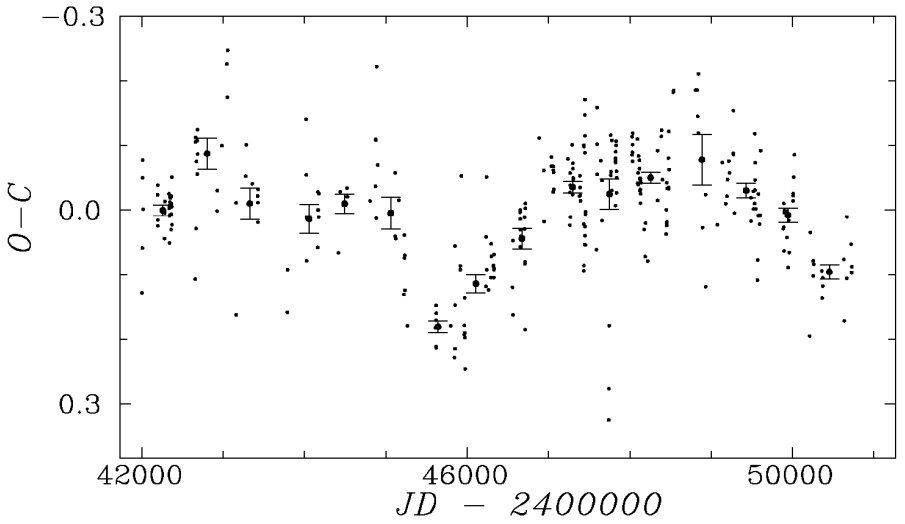


**Figure 6.** The $O-C$ deviations of the post-outburst B data consequently prewhitened to a linear trend and a trigonometric polynomial and to a best sine fit with $553^{\rm d}.1$ period.

## 4. The running parabolae fit and characteristics of individual cycles

As the individual cycles of variability may change their shape, we have used the method of running parabolae introduced by Andronov (1990) and recently extended to arbitrary basic and weight functions by Andronov (1997). For the fixed set of these functions, the only free parameter is the filter half–width $\Delta t$ which must be determined by computing the effective parameters of the fit for a grid of $\Delta t$. We have computed the error estimates $\sigma_1$ of the accuracy of one observation, ($\sigma_4$ ($= R\sigma_1$) in the notation of Andronov (1997)) and the signal to noise ratio $S/N$, which is equal to $\sigma_C/\sigma_4$. Here $\sigma_C$ is the r.m.s. deviations of the smoothed values from the mean.

Besides these parameters, Fig. 7 shows the dependencies of $\sigma_2$, $\sigma_5 = R\sigma_2$ (other estimates of $\sigma_1$ and $\sigma_4$, see Andronov (1997) for details), $R$ and $\sigma_3 = \sigma_{O-C}$ on $\Delta t$. One may note that the maximum of $S/N$ occurs at $\Delta t = 400^{\rm d}$, just where $\sigma_4$ reaches its minimum (neglecting differences of a few percent which are not very important for the fit). This value of $\Delta t$ is slightly smaller than that $0.545P = 521^{\rm d}$ expected for the harmonic signal with uncorrelated noise (Andronov, 1997). This is usual for signals with significant contributions of the harmonics of the main wave ($s > 1$) or for the signals with variable shape.

The two estimates $\sigma_1$ and $\sigma_2$ are very close to each other, justifying their good accuracy. The biased error estimate $\sigma_3$ is much smaller than $\sigma_1$ and $\sigma_2$ for small $\Delta t$, because of a smaller effective number of observations $n_e$ used for the local fit than for the larger $\Delta t$. The parameter $R$ monotonously decreases with $\Delta t$ as $n_e$ increases. All the parameters become asymptotically constant at $\Delta t$ exceeding the length of the interval of observations.

The corresponding dependencies for other bands show similar shapes and the values of $\Delta t$ corresponding to the maximal $S/N$ differ from the adopted value by a few percent, thus there is no need to use different values of $\Delta t$ for different data. The main characteristics for $\Delta t = 400^{\rm d}$ are listed in Table 3.

**Table 3.** Error estimates of the data $\sigma_1$, the fit $\sigma_4$ and the $S/N$ ratio for different data sets

| | U | B | V | pg | vis | AAVSO | AFOEV |
|---|---|---|---|---|---|---|---|
| $\sigma_1$ | $0\overset{\rm m}{.}138$ | $0\overset{\rm m}{.}078$ | $0\overset{\rm m}{.}085$ | $0\overset{\rm m}{.}189$ | $0\overset{\rm m}{.}242$ | $0\overset{\rm m}{.}234$ | $0\overset{\rm m}{.}224$ |
| $\sigma_4$ | $0\overset{\rm m}{.}046$ | $0\overset{\rm m}{.}026$ | $0\overset{\rm m}{.}028$ | $0\overset{\rm m}{.}039$ | $0\overset{\rm m}{.}023$ | $0\overset{\rm m}{.}025$ | $0\overset{\rm m}{.}027$ |
| $S/N$ | 14.0 | 19.1 | 16.3 | 14.8 | 15.8 | 14.9 | 14.5 |

Here we also include the sets from the AAVSO and AFOEV databases separately. As expected, the difference between the values of $\sigma_1$ is not very large (only 5%). The difference of $\sigma_4$ owes to the difference of $n_e$. However, it is strange that the "vis" data set, which is the unoverlapped sum of the AAVSO and AFOEV databases, corresponds to a larger value of $\sigma_1$. As an explanation,

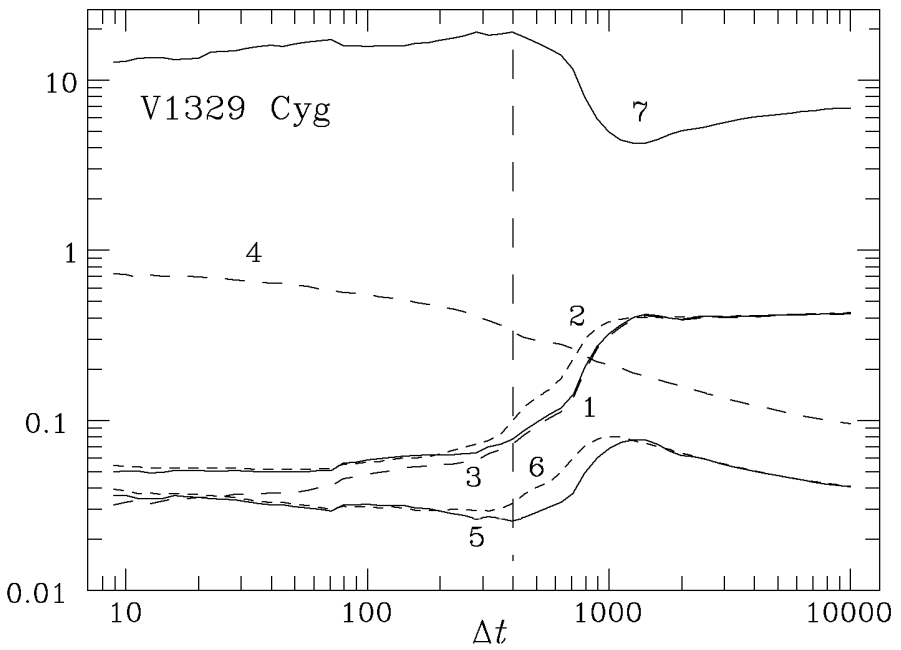


**Figure 7.** The dependence of the characteristics of the running parabola (RP) fit for the photoelectric B observations on $\Delta t$. The vertical line corresponds to the position of the local maximum at the $S/N$ curve: $\Delta t = 400^{\rm d}$. The lines correspond to: 1 ($\sigma_1$), 2 ($\sigma_2$), 3 ($\sigma_3 = \sigma_{O-C}$), 4 ($R$), 5 ($\sigma_4 = R\sigma_1$), 6 ($\sigma_5 = R\sigma_2$), 7 ($S/N = \sigma_C/\sigma_4$).

one may suggest the differences between the sequences of the comparison stars. However, this value is 10% smaller than for other stars, thus the data is of relatively low scatter.

The photographic data shows a larger value of $\sigma_1$ than that of the photoelectric observations because of their lower accuracy. However, the scatter is smaller than in the visual data because of the better homogeneity of the material used.

The characteristics of the extremes, determined by the method of running parabolae with the adopted filter half–width $\Delta t = 400^{\rm d}$ are listed in Tables 4 and 5. To compute the phases, we have used the ephemeris

$$JD_{min} = \underset{\pm 3}{2446771} + \underset{\pm 0.^{\rm d}6}{956.^{\rm d}5} \times E. \qquad (4)$$

The normal epoch of minimum and the period were computed as mean values from the values listed in Table 2 for U, B, V, vis and pg with weights proportional to inverse squares of the corresponding statistical errors, as usually assumed for the weighted mean (cf. Whittaker & Robinson 1926).

One may note in Figs. 2 and 3 the large deviations of the LC from the trigonometric polynomial trend before JD 2442000, where the fast decline and

**Table 4.** The U,B,V,pg extremes: time $T_e$ (-2400000), phase $\phi_e$ and magnitude $m_e$

| $T_e$ | $\phi_e$ | $m_e$ | $T_e$ | $\phi_e$ | $m_e$ |
|---|---|---|---|---|---|
| | U Max | | | U Min | |
| 40563 ±21 | 0.509±0.022 | 11.34±0.05 | 41276±28 | 0.255±0.029 | 12.96±0.05 |
| 41562 ± 4 | 0.554±0.004 | 11.48±0.19 | 41974± 8 | -0.015±0.008 | 13.21±0.05 |
| 42467 ± 4 | 0.500±0.004 | 11.73±0.03 | 42996±17 | 0.053±0.018 | 13.02±0.06 |
| 43452 ± 4 | 0.530±0.005 | 11.75±0.04 | 43815± 7 | -0.091±0.008 | 13.20±0.04 |
| 44422 ± 5 | 0.544±0.005 | 11.95±0.04 | 44865±15 | 0.008±0.016 | 13.52±0.08 |
| 45326 ±18 | 0.490±0.018 | 12.35±0.11 | 45871±13 | 0.059±0.014 | 13.82±0.04 |
| 46286 ±11 | 0.493±0.011 | 12.13±0.03 | 46808±22 | 0.038±0.023 | 13.59±0.05 |
| 47233 ± 6 | 0.483±0.007 | 12.08±0.05 | 47680±25 | -0.050±0.026 | 13.74±0.06 |
| 48227 ± 2 | 0.522±0.002 | 12.26±0.03 | 48641±10 | -0.045±0.011 | 13.80±0.05 |
| 49176 ±12 | 0.514±0.012 | 12.39±0.03 | 49638±18 | -0.003±0.019 | 13.86±0.02 |
| 50098 ± 4 | 0.478±0.004 | 12.41±0.03 | 50604± 7 | 0.008±0.007 | 14.22±0.05 |
| | B Max | | | B Min | |
| 40539 ±61 | 0.485±0.064 | 12.35±0.06 | 41306±26 | 0.287±0.028 | 13.61±0.07 |
| 41564 ± 6 | 0.557±0.007 | 12.82±0.13 | 41931±10 | -0.060±0.011 | 14.25±0.03 |
| 42462 ± 5 | 0.495±0.005 | 12.99±0.02 | 42936±36 | -0.010±0.038 | 14.02±0.05 |
| 43450 ± 3 | 0.528±0.003 | 12.90±0.02 | 43808±22 | -0.098±0.023 | 14.12±0.05 |
| 44416 ± 2 | 0.537±0.002 | 13.05±0.03 | 44837± 4 | -0.022±0.004 | 14.26±0.03 |
| 45269 ±31 | 0.430±0.033 | 13.42±0.02 | 45814± 5 | -0.000±0.005 | 14.57±0.04 |
| 46282 ±12 | 0.489±0.013 | 13.27±0.02 | 46771± 9 | -0.000±0.009 | 14.32±0.03 |
| 47234 ± 5 | 0.484±0.005 | 13.16±0.02 | 47697±12 | -0.032±0.012 | 14.38±0.03 |
| 48233 ± 2 | 0.528±0.002 | 13.38±0.01 | 48652±11 | -0.033±0.012 | 14.15±0.02 |
| 49172 ±11 | 0.510±0.011 | 13.43±0.02 | 49670± 2 | 0.031±0.002 | 14.58±0.04 |
| 50080 ± 8 | 0.459±0.008 | 13.51±0.03 | 50620± 6 | 0.024±0.006 | 14.70±0.03 |
| | V Max | | | V Min | |
| 40517 ±74 | 0.462±0.077 | 12.00±0.04 | 41065±31 | 0.034±0.033 | 13.16±0.10 |
| 41554 ±14 | 0.546±0.015 | 12.37±0.26 | 41910±19 | -0.082±0.020 | 13.55±0.04 |
| 42458 ± 5 | 0.491±0.006 | 12.46±0.02 | 42919±31 | -0.027±0.033 | 13.47±0.05 |
| 43442 ± 3 | 0.519±0.003 | 12.44±0.02 | 43783± 9 | -0.124±0.009 | 13.51±0.04 |
| 44435 ± 9 | 0.558±0.010 | 12.56±0.02 | 44829± 8 | -0.030±0.009 | 13.80±0.06 |
| 45252 ± 6 | 0.412±0.006 | 12.86±0.02 | 45806± 3 | -0.009±0.003 | 13.92±0.02 |
| 46266 ±14 | 0.472±0.015 | 12.72±0.02 | 46772±11 | 0.001±0.012 | 13.75±0.04 |
| 47232 ± 5 | 0.482±0.006 | 12.58±0.03 | 47719±12 | -0.009±0.013 | 13.83±0.03 |
| 48219 ±68 | 0.514±0.071 | 12.94±0.01 | 48682± 8 | -0.002±0.009 | 13.47±0.03 |
| 49157 ±12 | 0.494±0.013 | 12.92±0.02 | 49669± 2 | 0.030±0.002 | 14.05±0.05 |
| 50050 ±12 | 0.428±0.012 | 13.03±0.03 | | pg Min | |
| | pg Max | | 40019± 6 | -0.059±0.006 | 13.16±0.19 |
| 39323± 4 | 0.213±0.004 | 11.83±0.06 | 41138±44 | 0.111±0.046 | 13.37±0.06 |
| 40334±13 | 0.270±0.013 | 12.05±0.13 | 41887±86 | -0.106±0.089 | 14.00±0.07 |
| 41466±11 | 0.454±0.011 | 12.62±0.07 | 42950±48 | 0.006±0.050 | 14.18±0.14 |
| 43423± 8 | 0.499±0.008 | 13.05±0.02 | 43874± 4 | -0.028±0.004 | 14.32±0.04 |
| 44414± 6 | 0.536±0.007 | 13.15±0.02 | 44879± 8 | 0.022±0.008 | 14.44±0.02 |
| 45323± 8 | 0.486±0.008 | 13.34±0.04 | 45822±14 | 0.008±0.015 | 14.46±0.05 |
| 46312±10 | 0.520±0.010 | 13.26±0.09 | 46770± 8 | -0.001±0.009 | 14.45±0.04 |
| 47265±12 | 0.517±0.012 | 13.31±0.04 | 47733±32 | 0.006±0.034 | 14.47±0.05 |
| 48229± 9 | 0.525±0.010 | 13.41±0.04 | 48722±19 | 0.039±0.020 | 14.54±0.08 |

**Table 5.** The extremes based on the visual data: time $T_e$ (-2400000), phase $\phi_e$ and magnitude $m_e$

| $T_e$ | $\phi_e$ | $m_e$ | $T_e$ | $\phi_e$ | $m_e$ |
|---|---|---|---|---|---|
| | vis Max | | | vis Min | |
| 41533±18 | 0.524±0.019 | 12.89±0.03 | 41288± 8 | 0.268±0.009 | 13.27±0.04 |
| 42442±17 | 0.474±0.017 | 12.98±0.05 | 41948±10 | -0.042±0.011 | 13.62±0.02 |
| 43518± 5 | 0.599±0.005 | 12.64±0.04 | 42948±16 | 0.003±0.017 | 13.43±0.04 |
| 44528±47 | 0.655±0.049 | 13.08±0.07 | 44071±41 | 0.177±0.043 | 13.48±0.03 |
| 45469± 8 | 0.639±0.009 | 12.99±0.03 | 44878±15 | 0.021±0.016 | 13.45±0.03 |
| 46210± 5 | 0.414±0.005 | 12.53±0.03 | 45814±10 | -0.000±0.010 | 13.67±0.03 |
| 47275± 5 | 0.527±0.005 | 12.65±0.03 | 46811± 6 | 0.042±0.006 | 13.71±0.02 |
| 48182± 7 | 0.475±0.007 | 12.82±0.02 | 47719± 6 | -0.009±0.007 | 13.79±0.02 |
| 49191± 9 | 0.530±0.009 | 12.81±0.02 | 48681±11 | -0.003±0.011 | 13.68±0.02 |
| 50112± 6 | 0.493±0.006 | 13.27±0.02 | 49679± 3 | 0.040±0.004 | 13.93±0.01 |
| | | | 50590± 5 | -0.007±0.005 | 13.92±0.01 |

frequent outbursts were replaced by a relatively smooth curve with much smaller trend. Also, there are large distortions of the smoothing curve during the gaps causing apparent shifts of the extremes, e.g. near JD 2441300. The U and B LCs are highly distorted; the more dense photographic data shows an outburst that also shifts the LC.

However, the visual observations show much larger deviations from the periodic fit causing apparent huge changes to the shape of the light curve. One may note large apparent visual brightenings near JD 2446259 and 47368, despite the fact that photographic and photoelectric data show no evidence for them. This may be a result of the inhomogeneity of the observations and thus their larger scatter.

To look for possible phase shifts between the LCs in U,B,V bands we have chosen the extremes (either maxima or minima) determined in all three bands, neglecting those seen in one or two bands, only. The accuracy estimates of single data $\sigma$ were used for the weights $w = \sigma^{-2}$ (e.g. Whittaker & Robinson, 1926). The mean weights of the timings of the extremes correspond to $\sigma_t = 10\overset{\mathrm{d}}{.}7$, $5\overset{\mathrm{d}}{.}1$ and $4\overset{\mathrm{d}}{.}3$ for the U,B and V data, respectively. The weight of each difference was set to $w = w_1 w_2/(w_1 + w_2)$, because the variance of the difference between two uncorrelated variables is equal to the sum of the variances of these variables: $\sigma^2 = \sigma_1^2 + \sigma_2^2$ (e.g. Whittaker & Robinson, 1926). Here the indices 1 and 2 correspond to two colours in a pair. The mean differences between the times of extremes in different colours are $\langle t_U - t_B \rangle = 25^{\mathrm{d}} \pm 11^{\mathrm{d}}$, $\langle t_U - t_V \rangle = 30^{\mathrm{d}} \pm 16^{\mathrm{d}}$ and $\langle t_B - t_V \rangle = 12^{\mathrm{d}} \pm 5^{\mathrm{d}}$. A maximum near JD 2441280 was not taken into account as it was poorly defined. Thus one may conclude that all differences between the times of minima in different colours are equal to zero within corresponding error estimates.

**Table 6.** Photoelectric UBV observations of V1329 Cyg obtained at the Crimean station of the Sternberg Astronomical Institute.

| JD-2400000 | U | B | V | JD-2400000 | U | B | V |
|---|---|---|---|---|---|---|---|
| 47381 | 12.34 | 13.43 | 12.89 | 48119 | 12.30 | 13.46 | 12.97 |
| 47384 | 12.33 | 13.41 | 12.86 | 48121 | 12.36 | 13.47 | 12.99 |
| 47387 | 12.36 | 13.44 | 12.94 | 48124 | 12.35 | 13.48 | 13.02 |
| 47389 | 12.34 | 13.46 | 12.90 | 48127 | 12.31 | 13.47 | 13.05 |
| 47392 | 12.40 | 13.48 | 12.96 | 48128 | 12.30 | 13.45 | 13.02 |
| 47434 | 12.60 | 13.56 | 12.97 | 48129 | 12.28 | 13.45 | 13.00 |
| 47436 | 12.51 | 13.57 | 12.99 | 48131 | 12.29 | 13.48 | 12.99 |
| 47446 | 12.59 | 13.56 | 12.96 | 48133 | 12.29 | 13.46 | 13.00 |
| 47447 | 12.58 | 13.54 | 12.95 | 48134 | 12.33 | 13.44 | 12.99 |
| 47448 | 12.61 | 13.60 | 13.03 | 48176 | 12.38 | 13.41 | 12.91 |
| 47449 | 12.72 | 13.63 | 13.00 | 48188 | 12.43 | 13.43 | 12.93 |
| 47588 | 13.49 | 14.28 | 13.64 | 48193 | 12.36 | 13.37 | 12.92 |
| 47594 | 13.74 | 14.08 | 13.51 | 48218 | 12.33 | 13.40 | 12.92 |
| 47598 | - | 14.15 | 13.53 | 48340 | 12.39 | 13.38 | 12.95 |
| 47599 | 13.18 | 14.20 | 13.50 | 48341 | 12.35 | 13.46 | 13.12 |
| 47644 | 13.83 | 14.31 | 13.76 | 48387 | 12.62 | 13.50 | 13.01 |
| 47656 | 13.81 | 14.43 | 13.85 | 48390 | 12.67 | 13.50 | 12.97 |
| 47657 | 13.69 | 14.37 | 13.81 | 48400 | 12.77 | 13.61 | 13.04 |
| 47765 | - | 14.30 | 13.76 | 48446 | 13.13 | 13.86 | 13.21 |
| 47766 | 13.65 | 14.36 | 13.87 | 48448 | 13.20 | 13.83 | 13.22 |
| 47768 | 13.33 | 14.35 | 13.82 | 48450 | 13.20 | 13.86 | 13.23 |
| 47776 | 13.56 | 14.36 | 13.74 | 48451 | 13.23 | 13.80 | 13.19 |
| 47777 | 13.46 | 14.28 | 13.82 | 48452 | 13.26 | 13.87 | 13.22 |
| 47821 | 13.53 | 14.25 | 13.75 | 48456 | 13.29 | 13.88 | 13.24 |
| 47823 | 13.46 | 14.17 | 13.66 | 48459 | 13.32 | 13.84 | 13.26 |
| 47824 | 13.48 | 14.17 | 13.70 | 48473 | 13.35 | 13.85 | 13.24 |
| 47825 | 13.48 | 14.17 | 13.66 | 48474 | 13.35 | 13.90 | 13.25 |
| 47826 | 13.49 | 14.15 | 13.66 | 48476 | 13.33 | 13.91 | 13.25 |
| 47829 | 13.45 | 14.13 | 13.65 | 48478 | 13.34 | 13.83 | 13.23 |
| 47830 | 13.50 | 14.12 | 13.64 | 48483 | 13.51 | 13.91 | 13.29 |
| 47835 | 13.44 | 14.15 | 13.62 | 48532 | 13.49 | 14.01 | 13.37 |
| 47836 | 13.50 | 14.18 | 13.66 | 48539 | 13.51 | 14.04 | 13.43 |
| 47838 | 13.51 | 14.15 | 13.63 | 48809 | 13.57 | 14.08 | 13.45 |
| 48027 | 12.74 | 13.67 | 13.04 | 48827 | 13.49 | 14.00 | 13.34 |
| 48028 | 12.76 | 13.64 | 13.06 | 48834 | 13.54 | 14.01 | 13.32 |
| 48030 | 12.76 | 13.66 | 13.08 | 48840 | 13.71 | 14.01 | 13.37 |
| 48032 | 12.75 | 13.67 | 13.13 | 48842 | 13.39 | 13.91 | 13.28 |
| 48034 | 12.74 | 13.64 | 13.10 | 48892 | 13.54 | 13.96 | 13.40 |
| 48035 | 12.71 | 13.62 | 13.07 | 48930 | 13.31 | 13.80 | 13.18 |
| 48092 | 12.49 | 13.49 | 12.99 | 48931 | 13.33 | 13.94 | 13.19 |
| 48095 | 12.50 | 13.55 | 12.99 | 49075 | 12.52 | 13.55 | 13.02 |
| 48100 | 12.46 | 13.52 | 13.00 | 49134 | 12.34 | 13.38 | 12.87 |
| 48103 | 12.45 | 13.53 | 13.06 | 49178 | 12.35 | 13.44 | 12.94 |
| 48105 | 12.40 | 13.48 | 12.99 | 49194 | 12.39 | 13.44 | 12.94 |
| 48118 | 12.28 | 13.45 | 12.97 | 49200 | 12.39 | 13.42 | 12.96 |

**Table 6** (continued)

| JD-2400000 | U | B | V | JD-2400000 | U | B | V |
|---|---|---|---|---|---|---|---|
| 49215 | 12.40 | 13.41 | 12.87 | 49920 | 13.05 | 13.86 | 13.21 |
| 49223 | 12.37 | 13.44 | 12.92 | 49925 | 12.99 | 13.84 | 13.22 |
| 49270 | 12.49 | 13.50 | 13.03 | 49931 | 13.00 | 13.86 | 13.23 |
| 49273 | 12.52 | 13.44 | 12.99 | 49945 | 12.92 | 13.86 | 13.23 |
| 49274 | 12.49 | 13.51 | 13.03 | 49950 | 12.87 | 13.77 | 13.22 |
| 49287 | 12.66 | 13.63 | 13.07 | 49959 | 12.87 | 13.79 | 13.24 |
| 49490 | 13.70 | 14.15 | 13.56 | 50006 | 12.51 | 13.56 | 13.04 |
| 49491 | 13.75 | 14.19 | 13.61 | 50009 | 12.55 | 13.54 | 13.00 |
| 49517 | 13.72 | 14.25 | 13.65 | 50010 | 12.49 | 13.54 | 13.01 |
| 49520 | 13.69 | 14.29 | 13.69 | 50014 | 12.48 | 13.50 | 13.02 |
| 49534 | 13.74 | 14.34 | 13.68 | 50023 | 12.51 | 13.44 | 12.93 |
| 49536 | 13.63 | 14.24 | 13.67 | 50211 | 12.72 | 13.79 | 13.16 |
| 49538 | 13.70 | 14.32 | 13.75 | 50220 | 12.67 | 13.66 | 13.13 |
| 49539 | 13.81 | 14.34 | 13.77 | 50253 | 12.89 | 13.82 | 13.35 |
| 49542 | 13.74 | 14.31 | 13.78 | 50255 | 12.80 | 13.85 | 13.55 |
| 49549 | 13.74 | 14.41 | 13.87 | 50256 | 12.82 | 13.83 | 13.28 |
| 49567 | 13.90 | 14.59 | 14.02 | 50260 | 12.84 | 13.85 | 13.36 |
| 49570 | 13.88 | 14.57 | 14.02 | 50361 | 13.45 | 14.17 | 13.44 |
| 49578 | 13.81 | 14.53 | 13.94 | 50364 | 13.59 | 14.22 | 13.43 |
| 49582 | - | 14.51 | 13.97 | 50371 | 13.55 | 14.22 | 13.53 |
| 49596 | 13.84 | 14.60 | 14.16 | 50372 | 13.54 | 14.21 | 13.49 |
| 49601 | 13.81 | 14.60 | 14.12 | 50631 | 14.27 | 14.69 | 14.10 |
| 49609 | 13.84 | 14.52 | 14.02 | 50635 | 14.27 | 14.78 | 13.96 |
| 49886 | 13.34 | 14.00 | 13.36 | 50641 | 14.06 | 14.64 | 13.95 |
| 49891 | 13.29 | 13.98 | 13.39 | 50667 | 14.02 | 14.66 | 14.01 |
| 49892 | 13.29 | 13.94 | 13.34 | 50669 | 13.98 | 14.56 | 14.02 |
| 49896 | 13.28 | 14.00 | 13.36 | 50721 | 13.79 | 14.47 | 14.01 |
| 49901 | 13.21 | 13.92 | 13.30 | 50726 | 13.81 | 14.50 | 14.13 |
| 49902 | 13.25 | 13.92 | 13.30 | 50730 | 13.77 | 14.48 | 14.11 |

## 5. Conclusions

1. The ephemeris $\mathrm{JD}_{min}$ = 2 446 771(±3) + $956\overset{\mathrm{d}}{.}5(\pm 0\overset{\mathrm{d}}{.}6)\times E$ valid for post-outburst data.
2. The LCs in B and V are very similar with $\langle B-V\rangle = 0\overset{\mathrm{m}}{.}564 \pm 0\overset{\mathrm{m}}{.}005$ and a standard deviation from the mean of $\sigma_{B-V} = 0\overset{\mathrm{m}}{.}091$.
3. The variations in U have a larger amplitude ($1\overset{\mathrm{m}}{.}60$) and slope of the mean brightness ($10^{-4}$ mag/day) than in B,V ($1\overset{\mathrm{m}}{.}22$ and $7\ 10^{-5}$ mag/day, respectively).
4. The phase shifts of the minima in the U,B,V bands are within their error estimates.
5. The secondary wave with a period $553^{\mathrm{d}}$ and a semi-amplitude $0\overset{\mathrm{m}}{.}077 \pm 0\overset{\mathrm{m}}{.}007$ (B) may be present.

6. Long–term variations of the brightness with a cycle length $\approx 5300^{\rm d}$ and a semiamplitude $0\overset{\rm m}{.}084 \pm 0\overset{\rm m}{.}008$ (B) is suggested.

**Acknowledgements.** The authors are grateful to E. Schweitzer and the observers for their contribution to the AFOEV and AAVSO databases. This work has been partially supported by VEGA grants 1282/97 and 5038/98.

## References

Andronov, I.L.: 1990, *Kinem. Fiz. Nebesn. Tel* **6**, 87
Andronov, I.L.: 1994, *Odessa Astron. Publ.* **7**, 49
Andronov, I.L.: 1997, *Astron. Astrophys. Suppl.* **125**, 207
Arkhipova, V.P.: 1977, *Peremennye Zvezdy* **20**, 345
Arkhipova, V.P., Ikonnikova, N.P.: 1987, *Pisma Astron. Zh.* **15**, 140
Arkhipova, V.P., Mandel, O.E.: 1973, *Inf. Bull. Variable Stars* , No. 762
Arkhipova, V.P., Mandel, O.E.: 1991, *Pisma Astron. Zh.* **17**, 359
Bossen, H.: 1972, *Inf. Bull. Variable Stars* , No. 722
Dapergolas, A., Kontizas, E., Kontizas, M.: 1991, *Inf. Bull. Variable Stars* , No. 3583
Dumortier, B., Stram, E.: 1970, *Astronomie* **84**, 455
Gravina, R.: 1985, *Inf. Bull. Variable Stars* , No. 2834
Grygar, J., Hric, L., Chochol, D., Mammano, A.: 1979, *Bull. Astron. Inst. Czechosl.* **30**, 308
Hicks, P.D.: 1973, *Inf. Bull. Variable Stars* , 804
Hric, L., Skopal, A., Chochol, D., Komžík, R., Urban, Z., Papoušek, J., Blanco, C., Niarchos, P., Rovithis-Livaniou, H., Rovithis, P., Chinarova, L.L., Pikhun, A.I., Tsvetkova, K., Semkov, E., Velič, Z., Schweitzer, E.: 1994, *Contrib. Astron. Obs. Skalnaté Pleso* **24**, 31
Iijima, T., Mammano,A., Margoni,R.: 1981, *Astrophys. Space Sci.* **75**, 237
Kohoutek, L., Bossen, H.: 1970, *Astrophys. Lett.* **6**, 157
Munari, U., Margoni, R., Mammano, A.: 1988, *Astron. Astrophys.* **202**, 83
Mürset, U., Nussbaumer, H.: 1994, *Astron. Astrophys.* **282**, 586
Nussbaumer, H., Vogel, M.: 1991, *Astron. Astrophys.* **248**, 81
Richter, N.: 1972, *Inf. Bull. Variable Stars* , No. 708
Schild, H., Schmid, H.M.: 1997, *Astron. Astrophys.* **324**, 606
Schweitzer, E.: 1997, *ftp://cdsarc.u-strasbg.fr/pub/afoev/cyg/v1329*
Skopal, A.: 1998, *Astron. Astrophys.* **338**, 599
Skopal, A., Hric, L., Urban, Z., Pigulski, A., Blanco, C., Papoušek, J., Hanžl, D., Agerer, F., Niarchos, P., Rovithis-Livaniou, H., Rovithis, P., Tsvetkova, K., Semkov, E., Velič, Z., Michálek, F., Komačka, Ľ., Schweitzer, E., Korth, S.: 1992, *Contrib. Astron. Obs. Skalnaté Pleso* **22**, 131
Stienon, R.M., Chartrand, M.R. Shao, C.Y.: 1974, *Astron. J.* **79**, 47
Taranova, O.G., Yudin, B.F.: 1986, *Astron. Zh.* **63**, 151
Viotti, R., Hack, M.: 1993, *NASA SP* **507**, 663
Wehlau, W., Leung, K.-C.: 1964, *Astron. J.* **139**, 843
Whittaker, E., Robinson, G.: 1926, *The Calculus of Observations*, Blackies & Sons, London
Witzigmann, S., Kiehl, M., Hopp, U.: 1978, *Inf. Bull. Variable Stars* , No. 1463